Soft versus hard junction formation for α-terthiophene molecular wires and their charge transfer complexes

Andrea Vezzoli[a‡], Iain M. Grace[b‡], Carly Brooke[a], Richard J. Nichols[a], Colin J. Lambert[b] and Simon J. Higgins[a*]

a) Department of Chemistry, University of Liverpool, Crown Street, Liverpool L69 7ZD, UK
b) Quantum Technology Centre, Physics Department Lancaster University, Lancaster LA1 4YB, UK

‡ These authors contributed equally to this work

*Corresponding Author: shiggins@liverpool.ac.uk

This manuscript was accepted by J. Chem. Phys. Click here to see the version of record.

Abstract

We used a range of scanning tunnelling microscopy (STM)-based methods to conduct a detailed study of single molecule junction conductance enhancement upon charge transfer complex formation, using bis(thiaalkyl)arene molecular wires as electron donors, and tetracyanoethene (TCNE) as electron acceptor. Using the 'hard' STM break junction (STM-BJ) method, in which a Au STM tip is pushed into a Au substrate, and then withdrawn in the presence of molecules, we see a single, very broad, peak in the resulting conductance histogram when all data are used; the conductance enhancement is 25-fold for a terthiophene donor and 15-fold for a phenyl group. When rational data selection, in which only current-distance curves that contain a current plateau > 0.2 nm long are used in the conductance histogram, three sharper peaks are resolved in the histograms for the charge transfer complexes; two substantially lower-conductance peaks are resolved for the uncomplexed molecules. Using the 'soft' STM *I(s)* technique, in which initial contact between tip and substrate is avoided and the current limit is about an order of magnitude lower, we were able to resolve two peaks for the uncomplexed molecules depending upon the initial set point current (i.e. tip height), one at the same value as the lower of the two data-selected STM-BJ histogram peaks, and an additional peak beyond the low-current limit for the STM-BJ experiment. For the terthiophene, the low, medium and high conductance peaks for the TCNE complex are respectively *ca.* 70, 70 and 46 times higher in conductance than the corresponding peaks for the free molecule.

Introduction

Scanning probe microscopy techniques have played an important role in the development of methods for making and characterising metal / single molecule / metal junctions over the last 15 years. Among the most commonly-used methods today are the so-called scanning tunnelling microscopy break junction (STM-BJ), *I*(*s*) and *I*(*t*) (sometimes referred to as the STM 'blinking' or 'telegraph noise') methods.[1-6] The vast majority of studies have used gold substrates and STM tips. In the STM-BJ method, the STM tip is pushed into the substrate in the presence of a solution of target molecules, terminated at each end with a suitable contact group.[7] The tip is then withdrawn while the current is monitored, typically with a logarithmic amplifier owing to the extremely wide range of current characteristic of these experiments. As the resulting gold nanofilament thins and then breaks, steps down in current corresponding to the quantum unit of conductance G_0 are seen, until the final gold

point contact is broken. If one or more molecules become trapped between the broken point contacts, a characteristic region (or regions) in the current-vertical distance (*I*-s) trace is typically seen where the current is almost constant, referred to as a 'plateau', followed by another step down in current (this time much smaller than G_0) corresponding to the breakdown of the metal | molecule(s) | metal junction. Some typical STM-BJ traces obtained with thiol-contacted molecules are shown in Figure 1a.

In the *I(s)* and *I(t)* methods, contact between the tip and substrate is deliberately avoided. These methods are often performed with a sub-monolayer coverage of molecules already present on the substrate. In the *I(s)* method, the tip is brought to a predetermined height s_0 (using the setpoint current I_0 and bias V_{bias}) above the substrate, typically less than the length of the target molecule. The feedback loop is then disabled and the tip is withdrawn at a fixed rate while *I* is monitored. In a proportion of these experiments, a molecule spontaneously 'jumps' to form a metal /molecule / metal junction, and in such cases, on retraction the junction current *I* is greater at a given *s* than in the absence of a molecule, and plateau(s) are again apparent in the *I*-*s* curve prior to the junction breaking down. Following junction breakdown, the feedback loop is re-established and the tip is returned to s_0 prior to the next experiment. Some typical *I(s)* traces obtained with thiol-contacted molecules are shown in Figure 1b.

In the *I(t)* technique, the tip is also held at a predetermined s_0 but in this case it is not withdrawn. Instead, the feedback loop is disconnected and *I* is monitored for a fixed time *t*, typically up to 0.5 s, before feedback control is once more established. Sometimes a molecule will again spontaneously 'jump' to form a junction, whereupon *I* will increase by a characteristic amount, and then decrease by a similar amount as the junction spontaneously breaks. Some typical *I(t)* data obtained with thiol-contacted molecules are shown in Figure 1c.

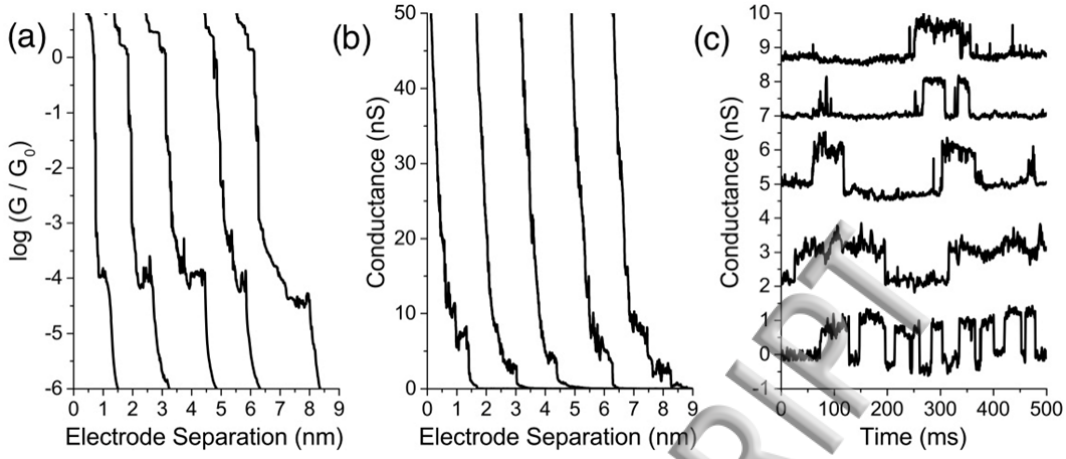

Figure 1: (a) Typical STM-BJ traces (as logarithm of quantum of conductance, shifted horizontally for clarity). (b) Typical *I(s)* traces (linear scale, shifted horizontally for clarity). (c) Typical *I(t)* traces (linear scale, shifted vertically for clarity).

In all of these methods, the stochastic nature of metal / molecule / metal junctions, the variable contact geometries open to most coordinating groups on the two metal surfaces (*q.v.*), and the likely torsional degrees of freedom of the molecule, all combine to make a range of metal / molecule / metal junction conductances inevitable. This, together with the fact that, in the tip withdrawal methods, a proportion of *I-s* traces are simply exponential decays with no evidence of junction formation, or are very noisy, perhaps as a result of tip contamination,[8] means that a statistical analysis of a large number of individual experiments has been an indispensible part of all STM-based studies of metal / single molecule / metal junctions. In the pioneering STM-BJ study (involving 4,4'-bipyridine and alkanedithiols $HS(CH_2)_nSH$; n = 6,8,10) the approach taken was to produce one-dimensional histograms by adding individual *I-s* traces and plotting current against frequency of observation of such a current.[7] The presence of plateaus at characteristic current values in individual *I-s* plots therefore results in characteristic peaks in the histogram. Although the criteria used to decide whether or not to include a particular *I-s* trace in the histograms were not then stated, in a later paper it was made clear that traces that did not contain clear plateau(x) (*i.e.* were simple exponential decays, or noisy with no discernable plateau) were not included.[9] Similarly, in early *I(s)* studies, only those *I-s* traces containing plateaus were analysed.[10] Since such histogram analysis often resulted in several peaks at roughly integer multiples of the lowest current peak, this was interpreted as the current plateaus in *I-s* traces being due to the formation of junctions involving integer numbers of molecules, with the lowest current

histogram peak (usually, significantly the most intense) logically corresponding to a single molecule junction.

A complicating factor was the early observation that different 'single molecule conductance' values were found for a given molecule by different groups, using apparently similar experimental and data analysis methods. To take one specific example, 1,8-octanedithiol, Xiao *et al*. first obtained a junction conductance of 2.5×10^{-4} G_0 using the STM-BJ method,[7] while Haiss *et al*. obtained a value of 1.3×10^{-5} G_0 using the *I(s)* technique.[11] Later, the Tao group reported that detailed analysis of a larger STM-BJ data set with a lower current minimum revealed a second, lower junction conductance value of 5.2×10^{-5} G_0 for this molecule.[12] Later, in a more complete study of 1,8-octanedithiol using both the STM-BJ and *I(s)* methods, as well as the matrix isolation method of Cui *et al*.[13] and the *I(t)* method[11], Haiss *et al*. showed that three different junction conductance values could be observed for 1,8–octanedithiol (2.3×10^{-4} G_0, 5.2×10^{-5} G_0 and 1.3×10^{-5} G_0), the prevalence of which depended upon the experimental conditions; in particular, there was an evident correlation between the degree of substrate surface roughness (assessed by STM imaging of an area prior to *I(s)* data collection), and the frequency of occurrence of the different conductance values.[14] This, together with the fact that higher–conductance junctions break down at shorter retraction distances, is consistent with the different conductance values corresponding to different possible contact geometries (both at step edges, or at least at sites where the Au contact atom has higher coordination; one at a step edge and the other flat, or both adsorbed at a flat site), with thiolate adsorbed to a Au step edge (or similar higher-coordination Au environment) giving a higher conductance.[1, 14] The most commonly-observed conductance value, when using the STM-BJ method or the *I(s)* method with relatively high set point current, *i.e*. relatively short initial tip-sample distance, was the intermediate value of $5.2 \times 10^{-5} G_0$. In all of the latter work, trace selection was used to construct the histograms; only those traces with clear plateaus were included in the analyses.

The use of trace selection in this manner has been criticised as leading to the possibility of observer bias.[15] Although a purely algorithm-based trace selection method did result in distinguishable histogram peaks for di-thiol molecules, these were notably less distinct than in previous work,[16] and in a later paper it was stated that STM-BJ data on di-thiols with all

data included did not result in any distinguishable conductance peak in one-dimensional histograms.[17] In contrast, it was found that similar STM-BJ experiments on molecules with amine (RNH_2) contact groups gave single, well-defined histogram peaks without any data selection. It was suggested that this was because the strong covalent Au-SR bond could result in many different possible junction configurations during individual *I-s* traces, whereas the weaker, dative Au-H_2NR bond resulted in stable junctions only when the Au contact atoms are undercoordinated, *i.e.* there is essentially only a single possible stable junction configuration. However, in notable contrast with this work, Chen *et al.* carried out a study of the effect of contact chemistry on the formation of single molecule junctions using their implementation of the STM-BJ method, comparing diamines, di-thiols and di-carboxylic acids of type $X(CH_2)_nX$ (X = $–NH_2$, –SH, –COOH), and found that all three families of molecules gave discernable histogram peaks, even when all current-distance traces (including 'molecule free' exponential decays and 'noisy' traces) were included in the analyses; in the latter instance, there was a notably worse signal-noise ratios but there were still conductance peaks at the same value. Moreover, all three types of contact groups gave two different conductance values ('high' and 'low' in their terminology), as observed already for di-thiols by the same group.[18] Other workers have made similar observations with both alkanedithiols[19] and conjugated dithiols,[20] although the detailed interpretation of the origin of the multiple conductance values has differed from group to group. Multiple conductance values have also been observed for other contact groups, for example amine-contacted oligophenyleneethynylenes,[21] simple α,ω-alkanedicarboxylic acids,[22] and 4–pyridyl-contacted systems *e.g.* 4–NC_5H_4-$(C{\equiv}C)_n$-C_5H_4N-4' (n = 1–4).[21, 23]

More recently (and subsequent to the period during which the data of this paper was collected), a novel experimental approach to fully–automated data collection and algorithm-based analysis using the *I(s)* technique has been developed, and the archetypal 1,8–octanedithiol was chosen as the first exemplar of this new method.[8] A junction conductance of $5 \times 10^{-5} G_0$ was observed, very similar to the 'medium' ('B' group) conductance previously determined, but the other conductance values were not distinct in their processed data. This is consistent with the observation of Haiss *et al.* that this conductance group is normally the most prevalent.[14]

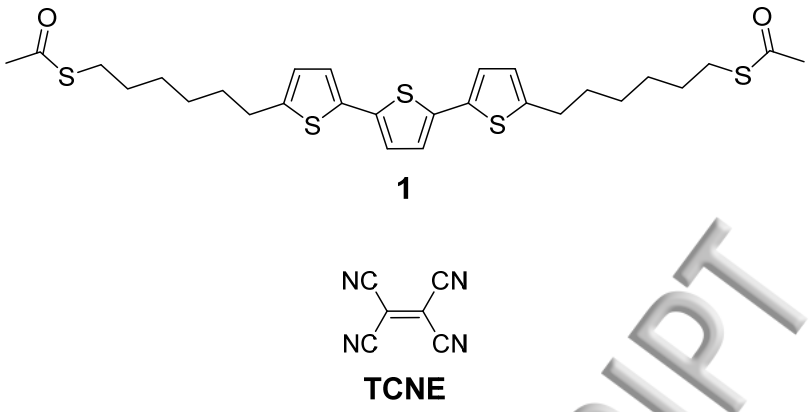

Figure 2: Structure of molecule **1** and TCNE.

We have recently described a substantial conductance increase for junctions involving molecule **1** (Figure 2) and related molecules upon charge transfer complex formation with the electron–deficient tetracyanoethylene (TCNE). For consistency between the two groups collaborating in this study, we used the STM-BJ method (without any data selection), although the resulting conductance histograms were extremely broad as is often the case with thiol contact groups. However, one issue with these very broad histograms, showing only a single peak, is that one cannot be sure whether the junctions involved are truly 'single molecule' in nature. This is a particularly pertinent issue in the present work; doping of polythiophene organic semiconductors with related (albeit more powerful) acceptors such as tetrafluoro–2,2'-(cyclohexa-2,5-diene-1,4-diylidene)dimalononitrile (F4TCNQ) has been studied in efforts to improve thin film transistor performance with these materials, and it has been shown that alternating donor-acceptor stacked aggregates form.[24] Therefore, we wished to test experimentally the possibility that the conductance boost seen for **1** with TCNE might be, at least in part, due to aggregate formation, *i.e.* that we see single molecule junctions in the absence of TCNE, but multiple molecule junctions owing to donor-acceptor stack interactions in the presence of TCNE.

Therefore, in the present work, we have used a combination of STM-BJ (with and without data selection), *I(s)* and *I(t)* methods to characterise further the interaction of **1** with TCNE. Using this approach, we find three distinct conductance values for **1** both in the presence and absence of TCNE; for the 'doped' system these all fall within the envelope of the single very broad peak previously seen in the STM-BJ experiments without trace selection, but in the case of **1** alone, only the two higher conductance

values fall within the envelope of the corresponding STM-BJ experiment broad peak; the third and lowest conductance value lies beyond the lower limit for the latter experiment, and it was necessary to use the *I(s)* technique with trace selection to determine this value. For this reason (and perhaps also as a result of the different distributions of the conductance events in the STM-BJ experiments in the presence and absence of TCNE), we therefore find significantly larger conductance increases for each conductance value in the presence of TCNE than was previously determined with the STM-BJ method alone, and we report these results here.

Results and discussion

In our previous work[25] we discussed the increase in conductance of a Au|**1**|Au junction upon exposure to an electron-deficient dopant. The observed phenomenon was attributed to the formation of a charge-transfer complex between the electron-rich α-terthiophene moiety incorporated in the molecular wire **1** and TCNE. All data shown in the paper was collected using the STM-BJ technique, and no selection was applied to the datasets: we collected thousands of current-distance traces as junctions were made and broken, and these were compiled in histograms with no further manipulation. As the hit rate (percentage of traces showing molecular bridging) lies between 10 and 30% for such experiments,[8] histograms were compiled including a large number of spurious traces, and this resulted in broad conductance peaks, spanning more than one order of magnitude. We reasoned that a process of rational data selection, removing all the traces that either bear no sign of junction formation, or show evident instrumental noise or anomalous current decay, may reveal a finer histogram peak structure, giving more information about junction formation, evolution and geometry. We therefore performed the same experiment (see Methods) using a higher-resolution, linear preamplifier (10 nA / V), and we selected only those traces with well-defined and long plateaux (> 0.2 nm), to be compiled into histograms.

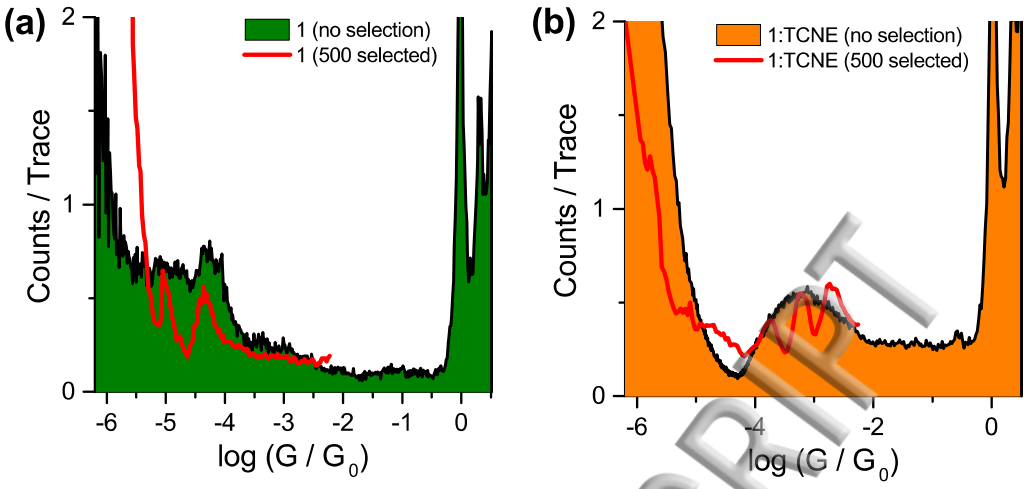

Figure 3: Comparison of dataset with (solid) and without (line) trace selection for **1** (a) and its complex with TCNE (b) obtained using the *STM-BJ* technique. Plots are normalised to counts / trace. Unselected data obtained with a logarithmic current follower. Selected data obtained with a linear, higher-resolution current follower (10 nA / V) but with a lower maximum current (100 nA).

Histograms obtained using the higher-sensitivity linear preamplifier after data selection are compared to the ones obtained using the logarithmic amplifier (also presented in our earlier work[25]) in Figure 3. It should be noted that since the linear amplifier had an upper current limit of 100 nA, we did not resolve the peaks at multiples of G_0 corresponding to the breaking of single Au atom contacts.

It is apparent from Figure 3 (b) that with data selection, there are three peaks in the conductance histogram within the conductance range sampled by the STM-BJ experiment using the linear preamplifier, and that these all fall within the single, broad peak seen in the earlier STM-BJ experiment without trace selection using the logarithmic amplifier. The observation of more than one conductance value for a single dithiol molecule (with trace selection) agrees with previous work on alkanedithiols[1, 12, 14, 19] and also on conjugated dithiols.[20] In this instance, the maximum in the unselected data (*ca.* $10^{-3}G_0$)[25] correlates well with the 'medium' (or 'B') conductance value (6.45×10^{-4} G_0; Table 1) in the selected data. However, in the absence of TCNE, the STM-BJ experiment with the linear preamplifier resolves only two peaks within its measureable range (Figure 3(a)), at $4.57 \times 10^{-5}G_0$ and $9.31 \times 10^{-6}G_0$ (Table 1) and the broad peak in the unselected data (*ca.* $5 \times 10^{-5}G_0$) roughly correlates with the *higher* of these two values.

This manuscript was accepted by J. Chem. Phys. Click here to see the version of record.

It is clear that for **1** in the presence of TCNE, the observed conductance values from the two experiments agree, but when no selection is applied to the dataset, contact information is lost and the various conductance contributions envelope into a single, broad feature in the histograms, but we observe only two peaks for uncomplexed **1**. We speculated that there could be a third, lower conductance value below the noise level of our instrument, and to test this idea, we repeated the experiment using the *I(s)* technique with a higher-resolution linear preamplifier (1 nA/V; upper current limit 10 nA). Using this preamplifier, we could resolve two conductance values, one ($2.56 \times 10^{-6} G_0$) below the minimum observable in the earlier experiments and the other ($8.91 \times 10^{-6} G_0$) correlating with the lower of the two values observed with the 100 nA preamplifier.

Table 1 summarises the data; the factors by which the three different conductance groups seen for uncomplexed **1** differ (from lowest to highest, 3.5 and 5.5) are similar but not identical to the factors typically observed for alkanedithiols (4.4 and 4.0 for 1,8-octanedithiol, for example[14]). Turning to the factor by which each conductance value is boosted by TCNE complexation, these are (from lowest conductance value to highest) respectively 72, 70 and 46 (using the means of STM-BJ and *I(s)* values where both are available). These factors are therefore significantly higher than the value (20 fold) found for the earlier STM-BJ data for **1**.[25] The observation of the three different conductance groups both in the presence and absence of TCNE is strong circumstantial evidence that in these experiments, we are indeed observing singe molecule junctions, because junctions involving multiple molecules bridging the tip and substrate would be likely to sample multiple different contact configurations and not give well-defined histogram peaks.

For alkanedithiols, Haiss *et al.* observed a correlation in *I(s)* experiments between the roughness of the substrate surface, and the frequency of occurrence of the higher conductance junctions.[14] Accordingly, we examined whether this applied to junctions with **1** and its TCNE complex. A sub-monolayer coverage of adsorbed **1** was employed, and the experiments were conducted under 1,2,4–trichlorobenzene, both in the presence and absence of 1 mM TCNE. In each case, before data collection the substrate surface was imaged until either a highly flat or a highly stepped area was located, and data collection was performed either only on highly–flat (RMS roughness < 0.4 nm) or only on highly–stepped areas (RMS roughness > 1 nm) until at least 500 I(s) traces containing plateaux had

been collected. The setpoint I_0 was chosen to ensure an initial tip-substrate separation < 1 nm (*i.e.* less than the length of **1**; *ca.* 2 nm S…S).

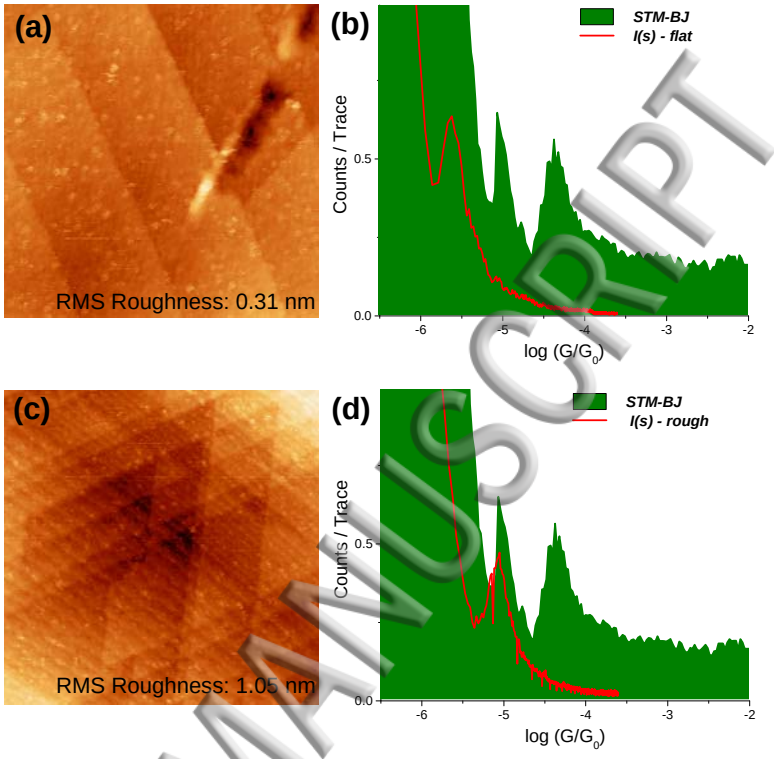

Figure 4: (a) Example of an STM image of low-stepped, low-roughness areas (I_0 = 1 nA, V_{BIAS} = –0.035 V). (b) Conductance histogram obtained from 500 successful molecular trapping in approach-withdrawal of the tip on low RMS roughness substrates (I_0 = 7 nA, V_{BIAS} = –0.3 V) with the *I(s)* technique (red line), and comparison with STM-BJ experiment (on substrate with undefined roughness, with data selection; solid green). (c) Example of an STM image of highly-stepped, high-roughness areas (I_0 = 1 nA, V_{BIAS} = –0.035 V). (d) Conductance histogram obtained from 500 successful molecular trapping in approach-withdrawal of high RMS roughness substrates (I_0 = 7 nA, V_{BIAS} = –0.3 V) with the *I(s)* technique (red line), and comparison with STM-BJ experiment (on substrate with undefined roughness, with data selection; solid green).

Figure 4 illustrates the results of these experiments for **1** in the absence of TCNE. It is evident that when *I(s)* scans are collected on highly–flat areas (Figure 4(a) and (b)), the lowest–conductance junctions are formed almost exclusively, whereas on highly–stepped areas, the medium conductance junctions are observed (Figure 4(c) and (d)). The experiments were repeated in the presence of 1 mM TCNE (Figure 5). Again, measurements on a low RMS roughness area permitted the measurement of the lowest contribution alone, and performing approach-withdrawal of the tip on a stepped area resulted in isolation of the medium conductance value. Results of the measured

conductance values using the two different techniques are reported in Table 1. This is an important result as it highlights that different junction types can result from surfaces with different roughness values, even for molecules more complex than alkanedithiols.[14] This shows an advantage of the *I*(*s*) technique; it can be deployed non-destructively on flat or stepped surface areas, whereas the in-situ BJ technique unavoidably locally damages flat surface regions due to the tip-to-surface metallic contact. However, it is interesting to note that the results obtained using the two different techniques are comparable (albeit the *I(s)* conductance values are consistently slightly lower).

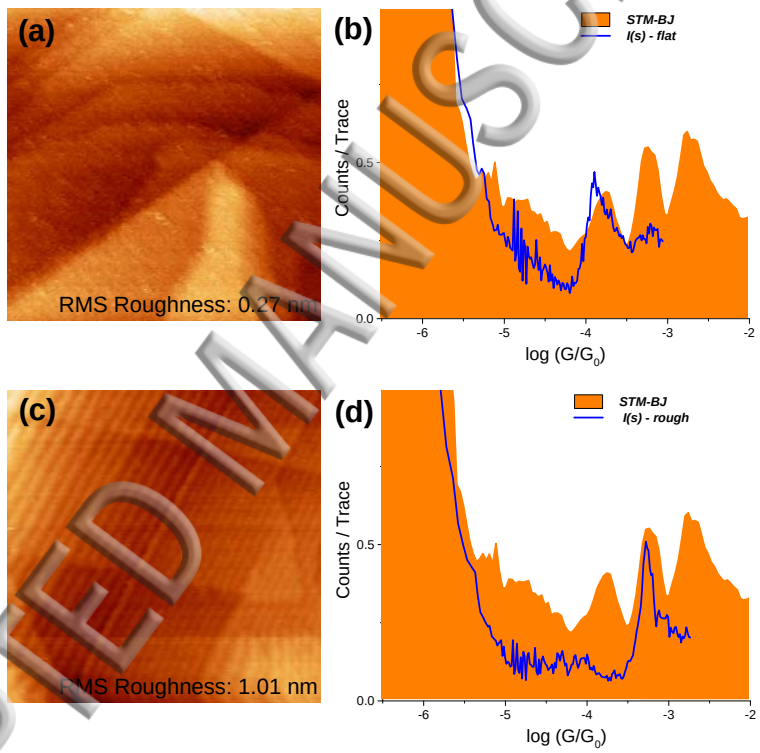

Figure 5: STM measurements in 10^{-3} M TCNE in 1,2,4-trichlorobenzene solution. (a) Example of a 200 x 200 nm STM image of low-stepped, low-roughness areas (I_0 = 1 nA, V_{BIAS} = –0.035 V). (b) Conductance histogram obtained from 500 successful molecular trapping of **1**:TCNE in approach-withdrawal of the tip on low RMS roughness substrates (I_0 = 20 nA, V_{BIAS} = –0.3 V) with the *I(s)* technique (blue line), and comparison with STM-BJ experiment (on substrate with undefined roughness, with data selection; solid orange). (c) Example of a 200 x 200 nm STM image of highly-stepped, high-roughness areas (I_0 = 1 nA, V_{BIAS} = –0.035 V). (d) Conductance histogram obtained from 500 successful molecular trapping of **1**:TCNE in approach-withdrawal of high RMS roughness substrates (I_0 = 60 nA, V_{BIAS} = –0.3 V) with the *I(s)* technique (blue line), and comparison with STM-BJ experiment (on substrate with undefined roughness, with data selection; solid orange).

	1 TCB *STM-BJ*	**1** TCB *I(s)*	**1** 10^{-3} M TCNE in TCB *STM-BJ*	**1** 10^{-3} M TCNE in TCB *I(s)*
G_{LOW}	--	2.56×10^{-6} G_0	1.90×10^{-4} G_0	1.78×10^{-4} G_0
G_{MEDIUM}	9.31×10^{-6} G_0	8.91×10^{-6} G_0	6.45×10^{-4} G_0	6.29×10^{-4} G_0
G_{HIGH}	4.57×10^{-5} G_0	--	2.09×10^{-3} G_0	--

Table 1: Summary of conductance values for **1** and **1**:TCNE using the 2 different techniques, V_{BIAS} = -0.3 V. See the ESI for the individual histograms and 2d density plots.

Theoretical Calculations

The experimental measurements show conductance groups that may be attributed to different binding geometries. Therefore, using a first principles approach to quantum transport calculations we present a theoretical model to rationalise this. In agreement with the experiments, this model predicts that the largest conductance enhancement due to charge transfer complexation occurs for the lowest-conductance configuration, due to pinning of the Fano resonance produced by charge transfer complexation at the Fermi energy.

Molecule **1** is not an archetypal 'molecular wire' as the thiol anchor groups are decoupled from the π-system of the central terthiophene unit by the n-hexyl chains. For more typical fully-conjugated 'molecular wires', high conductance groups have been attributed to step edges or ad-atoms where the gold electrodes directly couple to the pi-system of the molecule[23, 26] but this is unlikely to be the case with **1**. Any theoretical model to understand the contact dependence in molecular junctions suffers from the inherent difficulty in determining the geometry of the gold surface due to the dynamical nature of STM measurements. Therefore, in this work we assume idealised flat electrode surfaces of Au(111) for the calculations, as shown in Figure 6(a)**,** and calculate optimum binding locations for thiol groups on this surface.

Using density functional theory and the SIESTA code[27] we identify two possible binding locations for this scenario. The first is the typical 'hollow' coordination site, where the sulfur atom connects to three gold atoms at a distance of 2.35 Å. The computed binding

energy for this geometry is 1.1 eV. The second location is the 'top' site geometry where the sulfur connects directly above a single gold atom at a distance of 2.5 Å, with a weaker binding energy of 1.01 eV. As well as minimizing with contact distance, the optimum tilt angle (defined as the Au-C-S bond angle) is found to be 123° for top and 118° for hollow geometries. These two binding locations present three possible molecule junction geometries which we define as: Top-Top (where both leads are connected at the top site as shown in Figure 6(a), Top-Hollow (one lead connected to top site and one to the hollow site) and Hollow-Hollow.

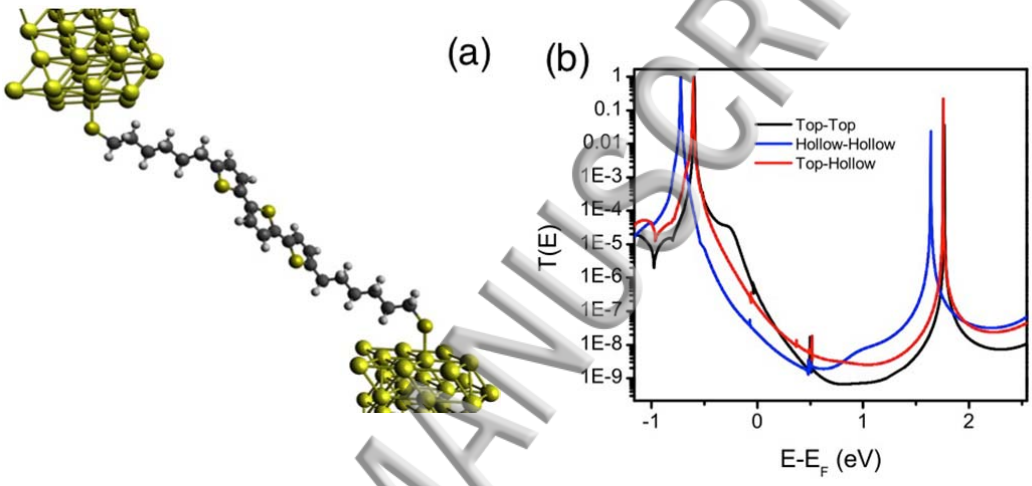

Figure 6. (a) Geometry of **1** in the molecular junction with terminal sulfur atoms contacted in a Top-Top configuration. (b) Zero-bias transmission coefficient for the three different contact geometries defined as Top-Top (black), Hollow-Hollow (blue) and Top-Hollow (red)

The molecular conductance was then calculated using the GOLLUM code[28] for the three different junction geometries, with the zero-bias transmission coefficients being shown in Figure 6(b). Here, the position of the Fermi energy (0 eV) shows that electron transport is through the tail of the HOMO resonance and the highest conductance ($G(E_F) = 3.2\times10^{-7}\,G_0$) occurs for the Top-Top binding geometry. This is due to two features, first, the shifting of the HOMO resonance closer to 0 eV and second, the appearance of an additional broad peak at approximately –0.25 eV for the Top-Top geometry, which is usually attributed to states localized on the terminal sulfur atoms (so-called 'gateway' states).[29] For the Hollow-Hollow configuration, at $E_F = 0$ eV the conductance is lowest ($G(E_F) = 2.0\times10^{-8}\,G_0$) as this extra peak has shifted to lower energy, leading to the HOMO resonance at –0.7 eV becoming more broadened. The Hollow-Top asymmetric coupling gives a conductance

This manuscript was accepted by J. Chem. Phys. Click here to see the version of record.

value of $G(E_F) = 1.3\times10^{-7}\,G_0$. This result shows that the peak, due to orbitals located on the sulfur atoms, is highly sensitive to the contact geometry and rationalises why multiple contact groups can be found in the experimental data. In this case, we can account for the three conductance groups by the variable coordination number of the sulfur atoms. The lowest conductance occurs when both contacts are coupled to three gold atoms and the highest when both are coupled to a single atom. The middle conductance group occurs for an asymmetric coupling.

We then test the conductance enhancement due to complexation with TCNE, using the optimum binding configuration found in the previous work.[25] The transmission curves shown in Figure 7 display a Fano resonance at 0 eV which, as described in the earlier work,[25] is due to the formation of the charge transfer complex. For the three different contact geometries there is little alteration in the position of the Fano peak, which means that in the region around the Fermi energy, the enhancement of the conductance is greatest for the Hollow-Hollow geometry. At a value of E-E_F = 0.06 eV the enhancement ratio is calculated as 53 for Top-Top, 102 for Top-Hollow and 150 for Hollow-Hollow. While these values are not fully in agreement with the experimental ratios calculated from the values in Table 1 (respectively, 70, 70 and 43) the qualitative behaviour is, and the differences can be attributed to the idealized nature of this model, which ignores geometrical fluctuations and temperature that have previously been shown to broaden out the sharp peak and anti-resonance of the Fano resonance.[25] The broadening of the Fano resonance leads to lower conductance values and therefore decreases the enhancement ratio.

Theoretically, we have shown that using an idealized model of an optimized molecular junction at zero temperature can describe qualitatively the experimental findings. The high, medium and low conductance values can be attributed to binding locations where the sulfur atom co-ordinates with either one or three gold atoms and therefore the nature of the gold surface may determine which of these are most likely. Upon complexation with TCNE, the position of the Fano resonance is pinned to the Fermi energy meaning that enhancement of the conductance is greatest for the configuration with lowest conductance.

This manuscript was accepted by J. Chem. Phys. Click here to see the version of record.

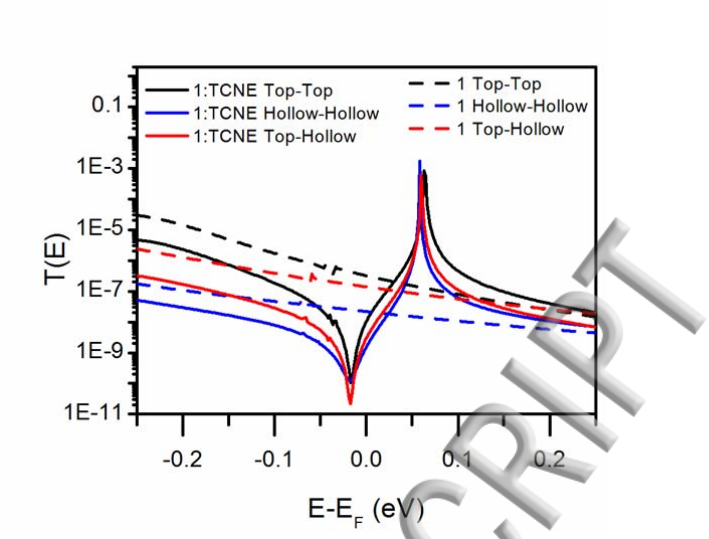

Figure 7. Transmission coefficient T(E) for 1:TCNE for the different binding geometries, top (black) and hollow (blue)

Methods

The synthesis of molecule **1** is described elsewhere.[25] All chemicals used throughout the experiments were purchased from Sigma-Aldrich Chemical Company and used as received. We used 11 × 11 mm gold on glass samples (Arrandee GmbH), that were flame annealed with a Bunsen burner immediately prior to sub-monolayer deposition. The annealing process involves heating the sample held at ~45° in the flame until it glows red and then keeping it glowing for 10 s by moving it in and out of the flame. The sample is then allowed to cool down for 30 s and the process is repeated three times before adsorption from 0.1 mM solutions of **1** in CH_2Cl_2. The thioacetate protecting group is spontaneously cleaved on contact with gold in the presence of ambient water.[1] The Au slide with a sub-monolayer of **1** is transferred to the STM sample holder and covered with 1,2,4-trichlorobenzene, with or without 1 mM TCNE, depending on the experiment. Molecular junctions are then formed *in situ* with an STM (former Molecular Imaging PicoSPM I, now Keysight 4500 SPM, Keysight Technologies Ltd.), equipped with a freshly-cut gold tip (Goodfellow Cambridge Ltd., UK - 99.99+ %, 0.25 mm), during the conductance measurements, using either the *I(s)*[10] or the STM-BJ[7] technique.

In the *I(s)* method, the tip is driven towards the surface until a desired setpoint current is reached, and then withdrawn at a speed of 40 nm s^{-1} while maintaining a constant *x-y* position and tip-substrate bias (V_{BIAS}). During the withdrawal a current-distance (*I*-s) curve is recorded. As no physical contact between the tip and the substrate is made in this

technique, surface roughness is not altered during an experiment, and the tip is maintained sharp. The substrate is routinely monitored by imaging the surface during the measurements. In the STM-BJ technique, the tip is pushed into the surface before withdrawal, using otherwise the same conditions employed in the *I(s)* technique. In both cases, a molecule can bridge the tip-substrate gap during the withdrawal process, and if this happens, a characteristic shape is observed in the current-distance traces: the current decreases with distance to settle at a plateau, typical of conductance through the extended molecule, and then it abruptly decays to zero when the tip is further withdrawn and the metal|molecule|metal junction is broken. The experimental break-off distance must be reasonably consistent with the length of the molecule (2.98 nm Au-molecule-Au for **1**) to provide confirmation that we are dealing with molecular events. Many current-distance traces bearing signs of molecular bridging are recorded, the conductance ($G = I / V_{BIAS}$) is calculated for the bare traces and the results are compiled in histograms to determine conductance values. The occurrence of plateaux in *I(s)* and STM-BJ traces results in peaks in the conductance histograms. The hit rate (percentage of scans showing a clear plateau) is usually in the range 5 - 10% of retraction events for the *I(s)* technique and 10 - 25 % for the STM-BJ technique; when data selection was applied, curves that did not show evidence of bridge formation (plateau-like features at least 0.2 nm long, extending beyond the tunnelling current decay in absence of molecule, ≈ 0.8 nm, with clear break-off) were discarded and not included in the histograms. The same traces were compiled into 2-dimensional density plots, with a correction for the experimentally-determined tip-sample separation (z_0) before tip withdrawal.[30] Additional histograms and 2-d plots for **1** and its charge-transfer complexes can be found in the ESI.

To perform the theoretical calculations, the molecules were relaxed with the SIESTA code, using a double-ζ plus polarization orbitals basis set until all the forces on the atoms were less than 0.01 eV/Ang. The local density approximation was used for the exchange correlational functional, with norm conserving pseudopotentials and a cut-off of 150 Rydbergs describing the real-space grid. To calculate the conductance an extended molecule approach was taken, with 6 layers of (111) gold each containing 9 gold atoms added to each electrode. The zero-bias transmission coefficient T(E) was then calculated using the Gollum code.

Conclusions

The results of this study highlight the possible advantages underlying the filtering of data in single molecule junction experiments, and the benefits of the non-contact *I(s)* technique, particularly for low–conductance junctions. Taken together, these approaches have enabled the refinement of our observation of a conductance increase for molecules of the structural type **1** upon charge transfer complex formation. We are now using this experimental approach to examine structure-property relations in this area, in particular the effects of varying the acceptor and donor moieties, and the length of the alkyl linkers.

Supplementary material

Supplementary material (additional linear one-dimensional and two-dimensional histograms, and additional theoretical data) is available at …. Experimental data is available on the data catalog in Liverpool at the address: http://datacat.liverpool.ac.uk/id/eprint/203

Acknowledgements

We thank EPSRC (grants EP/H035184/1 and EP/H035818/1) for funding.

References

1. R. J. Nichols, W. Haiss, S. J. Higgins, E. Leary, S. Martin and D. Bethell, Physical Chemistry Chemical Physics **12** (12), 2801-2815 (2010).
2. R. J. Nichols and S. J. Higgins, in *Annual Review of Analytical Chemistry, Vol 8*, edited by R. G. Cooks and J. E. Pemberton (2015), Vol. 8, pp. 389-417.
3. C. C. Huang, A. V. Rudnev, W. J. Hong and T. Wandlowski, Chemical Society Reviews **44** (4), 889-901 (2015).
4. S. V. Aradhya and L. Venkataraman, Nature Nanotechnology 8 (6), 399-410 (2013).
5. F. Chen and N. J. Tao, Accounts of Chemical Research **42** (3), 429-438 (2009).
6. J. Hihath and N. J. Tao, Semiconductor Science and Technology **29** (5) (2014).
7. B. Q. Xu and N. J. J. Tao, Science **301** (5637), 1221-1223 (2003).
8. M. S. Inkpen, M. Lemmer, N. Fitzpatrick, D. C. Milan, R. J. Nichols, N. J. Long and T. Albrecht, Journal of the American Chemical Society **137** (31), 9971-9981 (2015).
9. X. Y. Xiao, B. Q. Xu and N. J. Tao, Nano Letters **4** (2), 267-271 (2004).
10. W. Haiss, H. van Zalinge, S. J. Higgins, D. Bethell, H. Höbenreich, D. J. Schiffrin and R. J. Nichols, J. Am. Chem. Soc. **125**, 15294-15295 (2003).
11. W. Haiss, R. J. Nichols, H. van Zalinge, S. J. Higgins, D. Bethell and D. J. Schiffrin, Phys. Chem. Chem. Phys. **6**, 4330-4337 (2004).
12. X. L. Li, J. He, J. Hihath, B. Q. Xu, S. M. Lindsay and N. J. Tao, Journal of the American Chemical Society **128** (6), 2135-2141 (2006).
13. X. D. Cui, A. Primak, J. Tomfohr, O. F. Sankey, A. L. Moore, T. A. Moore, D. Gust, G. Harris and S. M. Lindsay, Science **294**, 571-574 (2001).
14. W. Haiss, S. Martin, E. Leary, H. van Zalinge, S. J. Higgins, L. Bouffier and R. J. Nichols, Journal of Physical Chemistry C **113** (14), 5823-5833 (2009).
15. M. Frei, S. V. Aradhya, M. S. Hybertsen and L. Venkataraman, Journal of the American Chemical Society **134** (9), 4003-4006 (2012).
16. J. Ulrich, D. Esrail, W. Pontius, L. Venkataraman, D. Millar and L. H. Doerrer, Journal of Physical Chemistry B **110** (6), 2462-2466 (2006).
17. L. Venkataraman, J. E. Klare, I. W. Tam, C. Nuckolls, M. S. Hybertsen and M. L. Steigerwald, Nano Letters **6** (3), 458-462 (2006).
18. F. Chen, X. L. Li, J. Hihath, Z. F. Huang and N. J. Tao, Journal of the American Chemical Society **128** (49), 15874-15881 (2006).
19. E. Pires, J. E. Macdonald and M. Elliott, Nanoscale **5** (19), 9397-9403 (2013).
20. V. Kaliginedi, P. Moreno-Garcia, H. Valkenier, W. Hong, V. M. Garcia-Suarez, P. Buiter, J. L. H. Otten, J. C. Hummelen, C. J. Lambert and T. Wandlowski, Journal of the American Chemical Society **134** (11), 5262-5275 (2012).
21. W. Hong, D. Z. Manrique, P. Moreno-Garcia, M. Gulcur, A. Mishchenko, C. J. Lambert, M. R. Bryce and T. Wandlowski, Journal of the American Chemical Society **134** (4), 2292-2304 (2012).
22. S. Martín, W. Haiss, S. J. Higgins, P. Cea, M. C. López and R. J. Nichols, J. Phys. Chem. C **112**, 3941-3948 (2008).
23. C. Wang, A. S. Batsanov, M. R. Bryce, S. Martin, R. J. Nichols, S. J. Higgins, V. M. Garcia-Suarez and C. J. Lambert, Journal of the American Chemical Society **131** (43), 15647-15654 (2009).

24. L. Müller, D. Nanova, T. Glaser, S. Beck, A. Pucci, A. K. Kast, R. R. Schröder, E. Mankel, P. Pingel, D. Neher, W. Kowalsky and R. Lovrincic, Chem. Mater. **28**, 4432-4439 (2016).
25. A. Vezzoli, I. Grace, C. Brooke, K. Wang, C. J. Lambert, B. Xu, R. J. Nichols and S. J. Higgins, Nanoscale **7** (45), 18949-18955 (2015).
26. W. Haiss, C. S. Wang, I. Grace, A. S. Batsanov, D. J. Schiffrin, S. J. Higgins, M. R. Bryce, C. J. Lambert and R. J. Nichols, Nature Materials **5** (12), 995-1002 (2006).
27. J. M. Soler, E. Artacho, J. D. Gale, A. Garcia, J. Junquera, P. Ordejon and D. Sanchez-Portal, Journal of Physics-Condensed Matter **14** (11), 2745-2779 (2002).
28. J. Ferrer, C. J. Lambert, V. M. Garcia-Suarez, D. Z. Manrique, D. Visontai, L. Oroszlany, R. Rodriguez-Ferradas, I. Grace, S. W. D. Bailey, K. Gillemot, H. Sadeghi and L. A. Algharagholy, New J. Phys. **16**, 093029 (093016 pp) (2014).
29. F. Huser and G. C. Solomon, Journal of Physical Chemistry C **119** (25), 14056-14062 (2015).
30. G. Sedghi, K. Sawada, L. J. Esdaile, M. Hoffmann, H. L. Anderson, D. Bethell, W. Haiss, S. J. Higgins and R. J. Nichols, J. Am. Chem. Soc. **130**, 8582-8583 (2008).

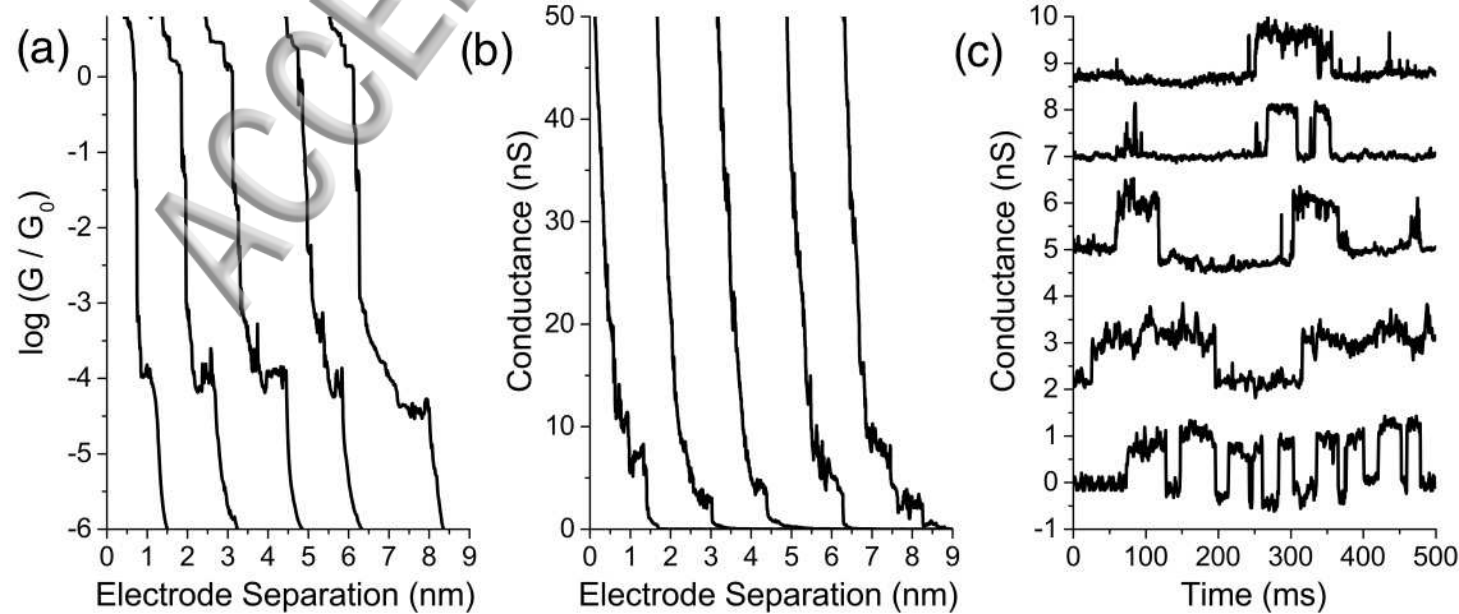
(a)
log (G / G0)
Electrode Separation (nm)
(b)
Conductance (nS)
Electrode Separation (nm)
(c)
Conductance (nS)
Time (ms)

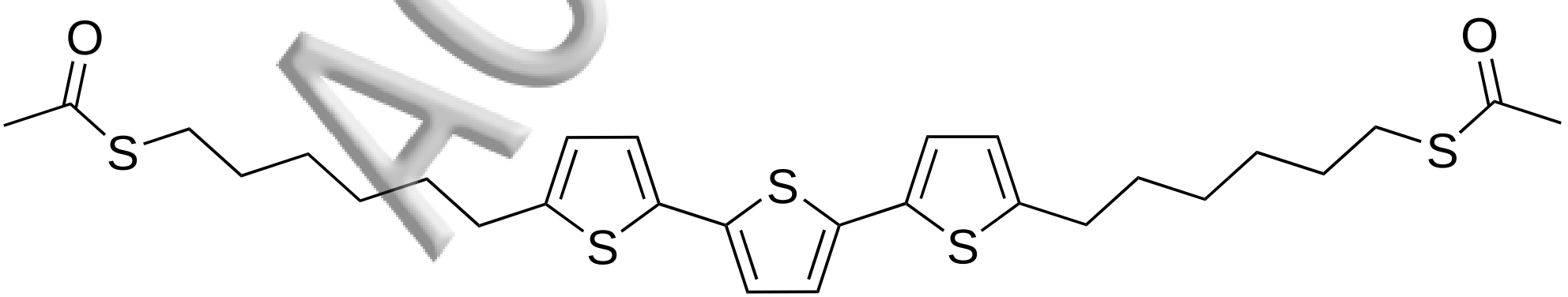

1

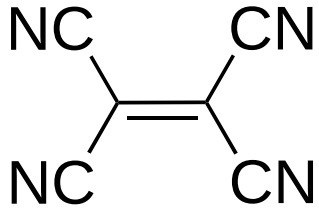

TCNE

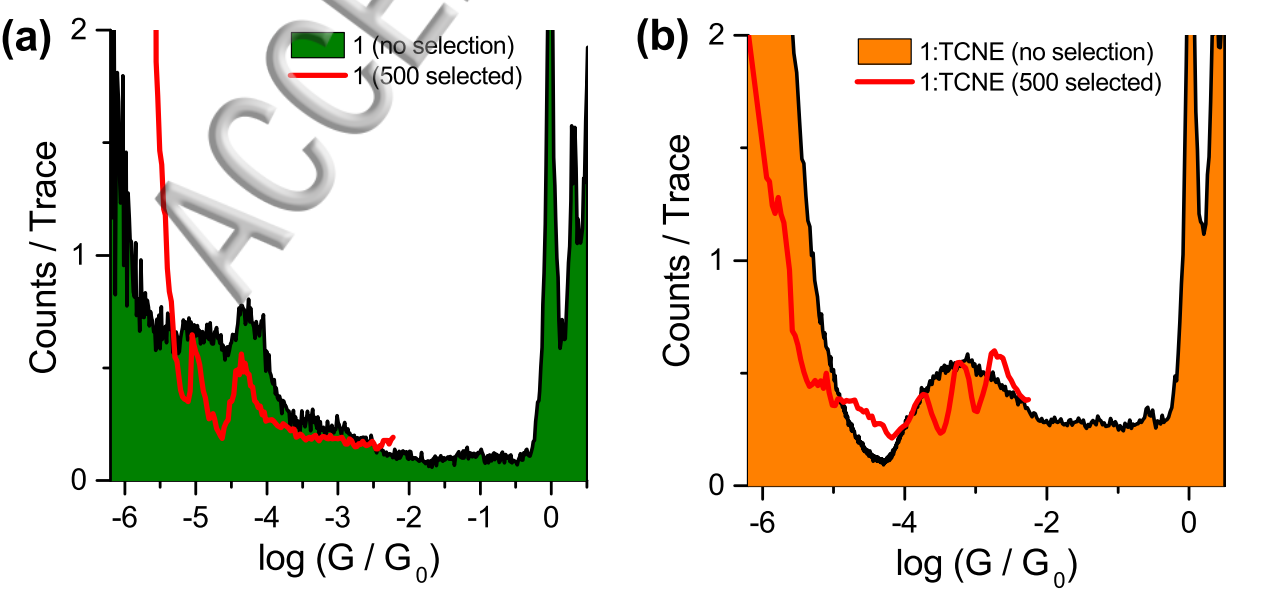
(a)
1 (no selection)
1 (500 selected)
Counts / Trace
log (G / G0)
(b)
1:TCNE (no selection)
1:TCNE (500 selected)
Counts / Trace
log (G / G0)

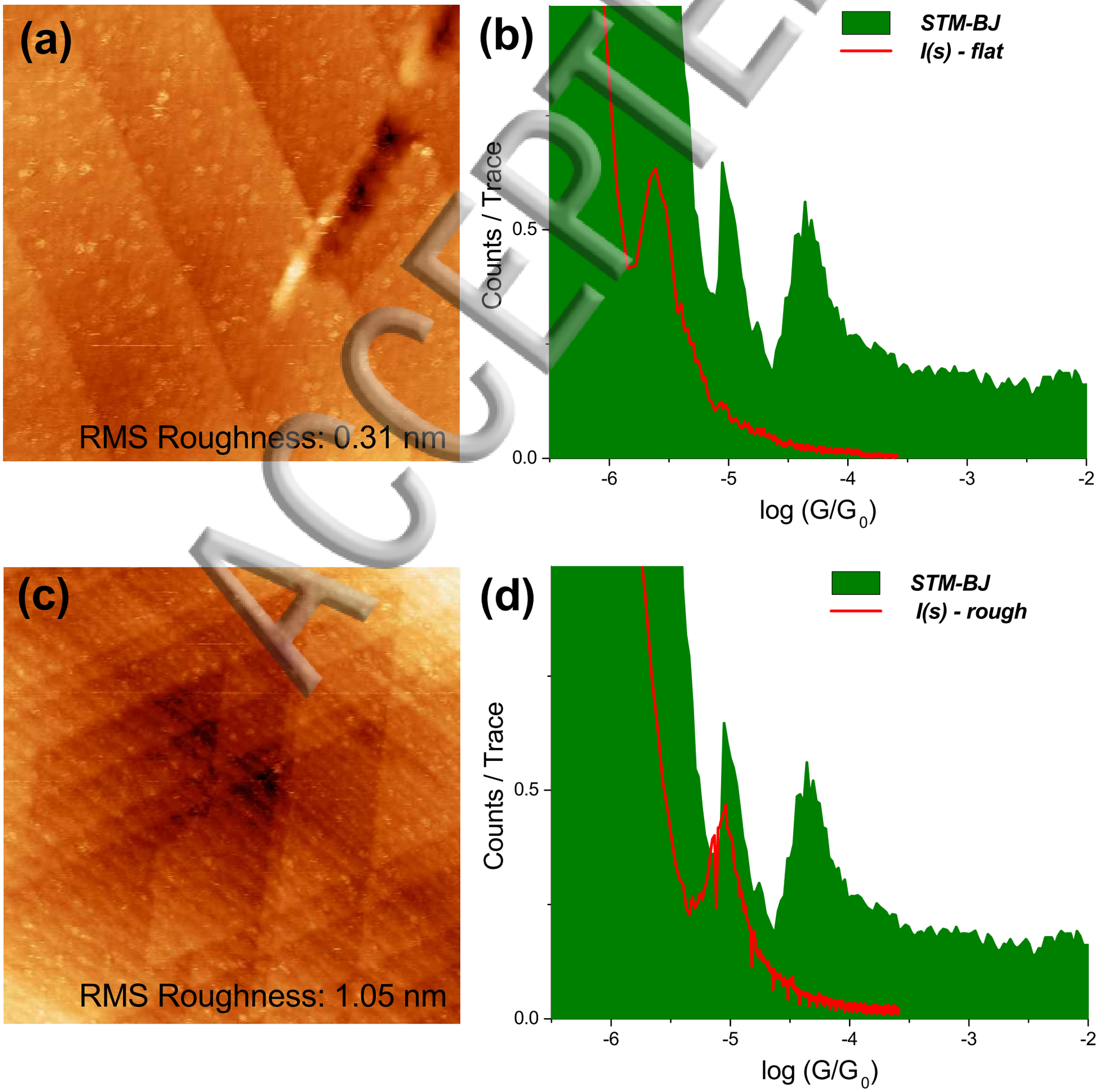
(a)
RMS Roughness: 0.31 nm
(b)
STM-BJ
I(s) - flat
Counts / Trace
0.5
0.0
-6
-5
-4
-3
-2
log (G/G0)
(c)
RMS Roughness: 1.05 nm
(d)
STM-BJ
I(s) - rough
Counts / Trace
0.5
0.0
-6
-5
-4
-3
-2
log (G/G0)

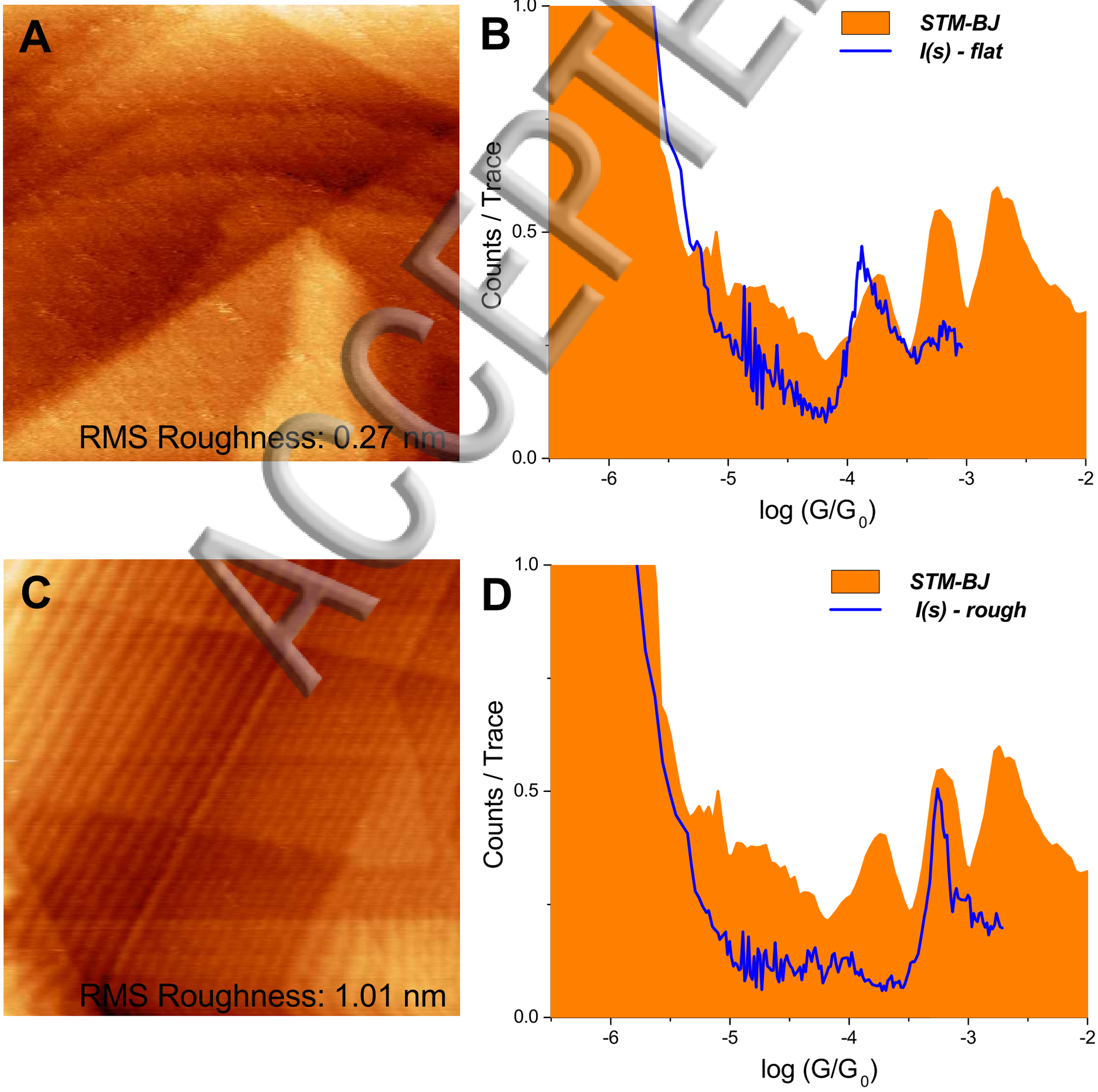
A
RMS Roughness: 0.27 nm
B
STM-BJ
I(s) - flat
Counts / Trace
1.0
0.5
0.0
-6
-5
-4
-3
-2
log (G/G0)
C
RMS Roughness: 1.01 nm
D
STM-BJ
I(s) - rough
Counts / Trace
1.0
0.5
0.0
-6
-5
-4
-3
-2
log (G/G0)

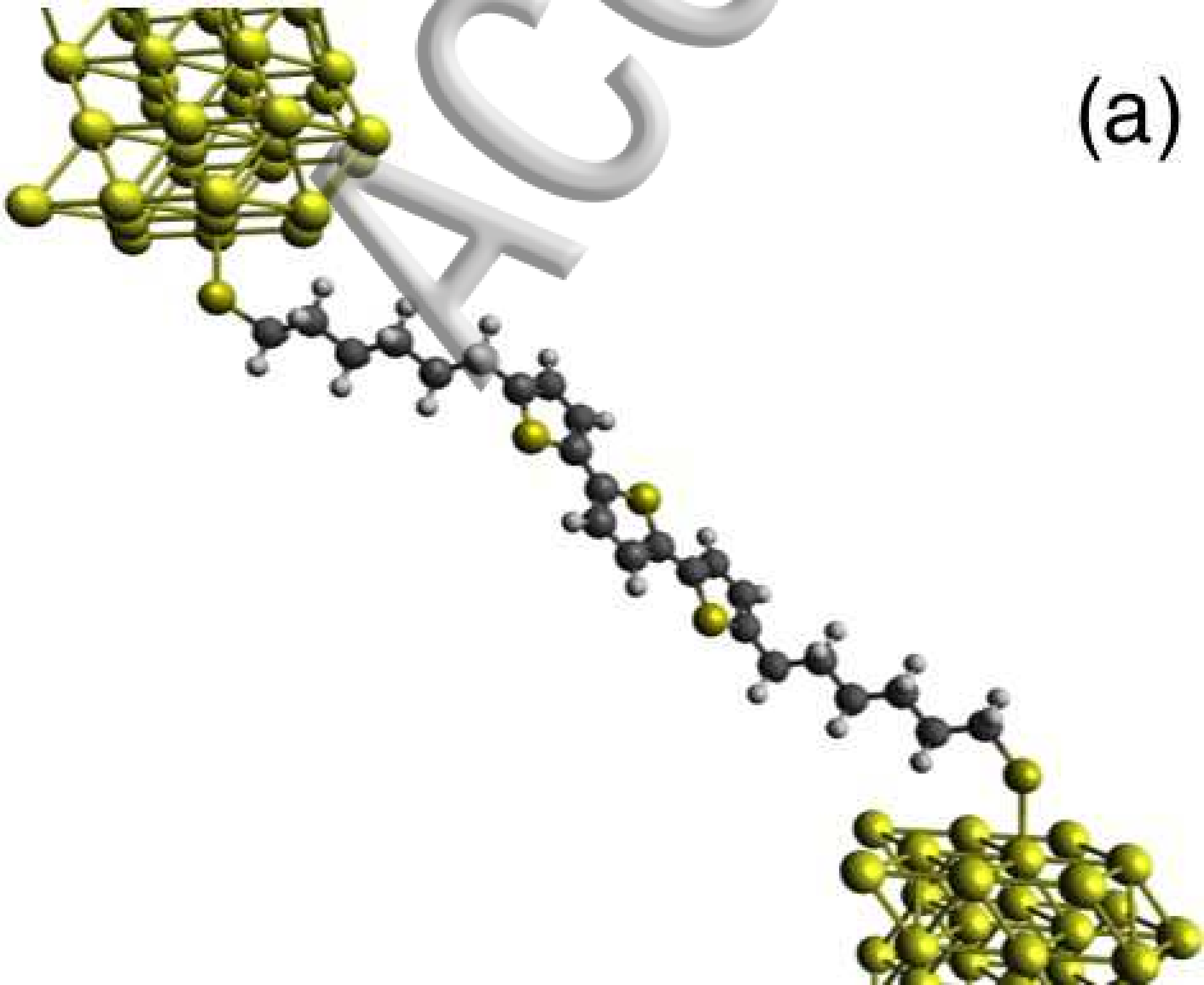
(a)

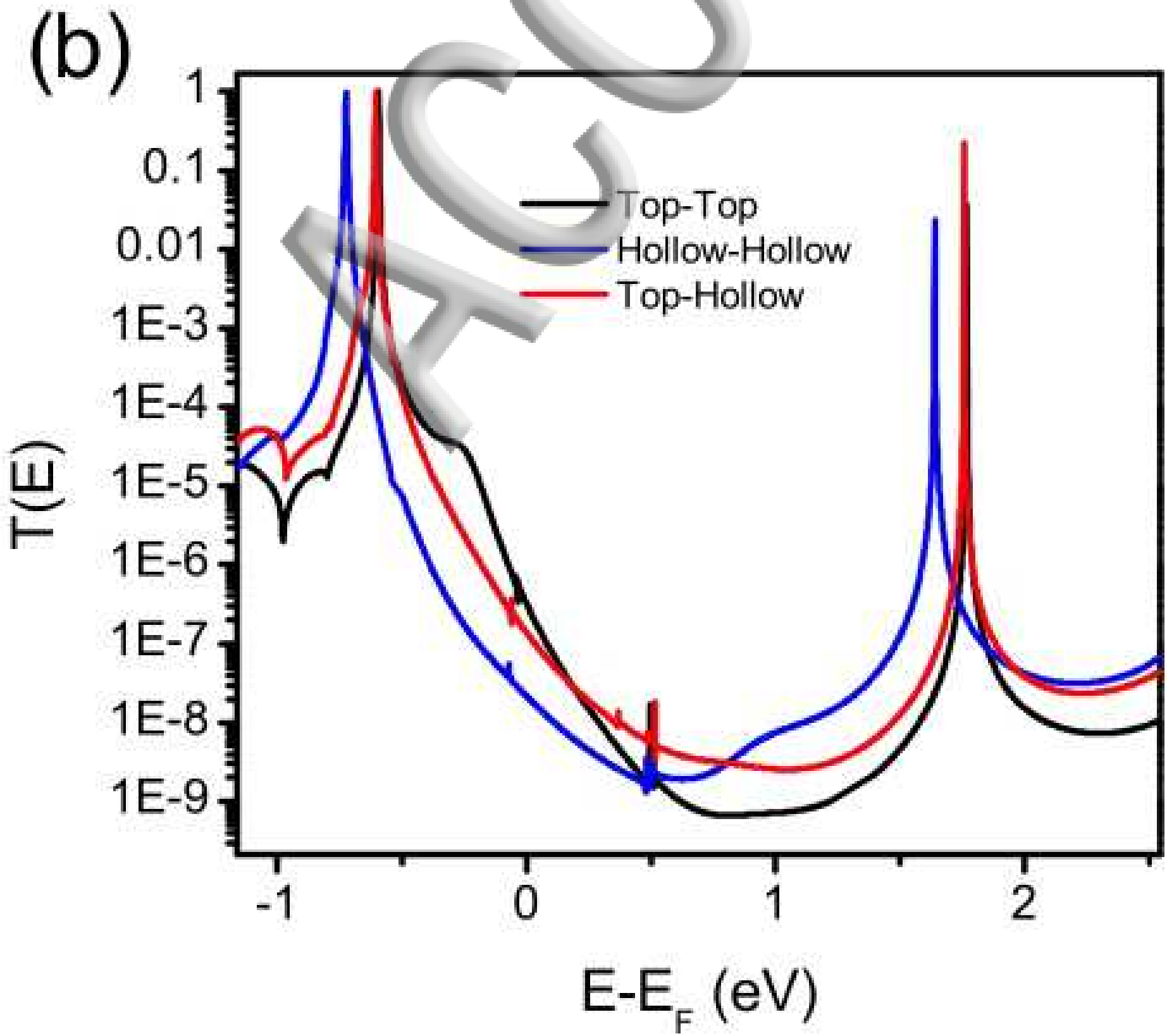
(b)
1
0.1
0.01
1E-3
1E-4
1E-5
1E-6
1E-7
1E-8
1E-9
T(E)
Top-Top
Hollow-Hollow
Top-Hollow
-1
0
1
2
E-E$_F$ (eV)

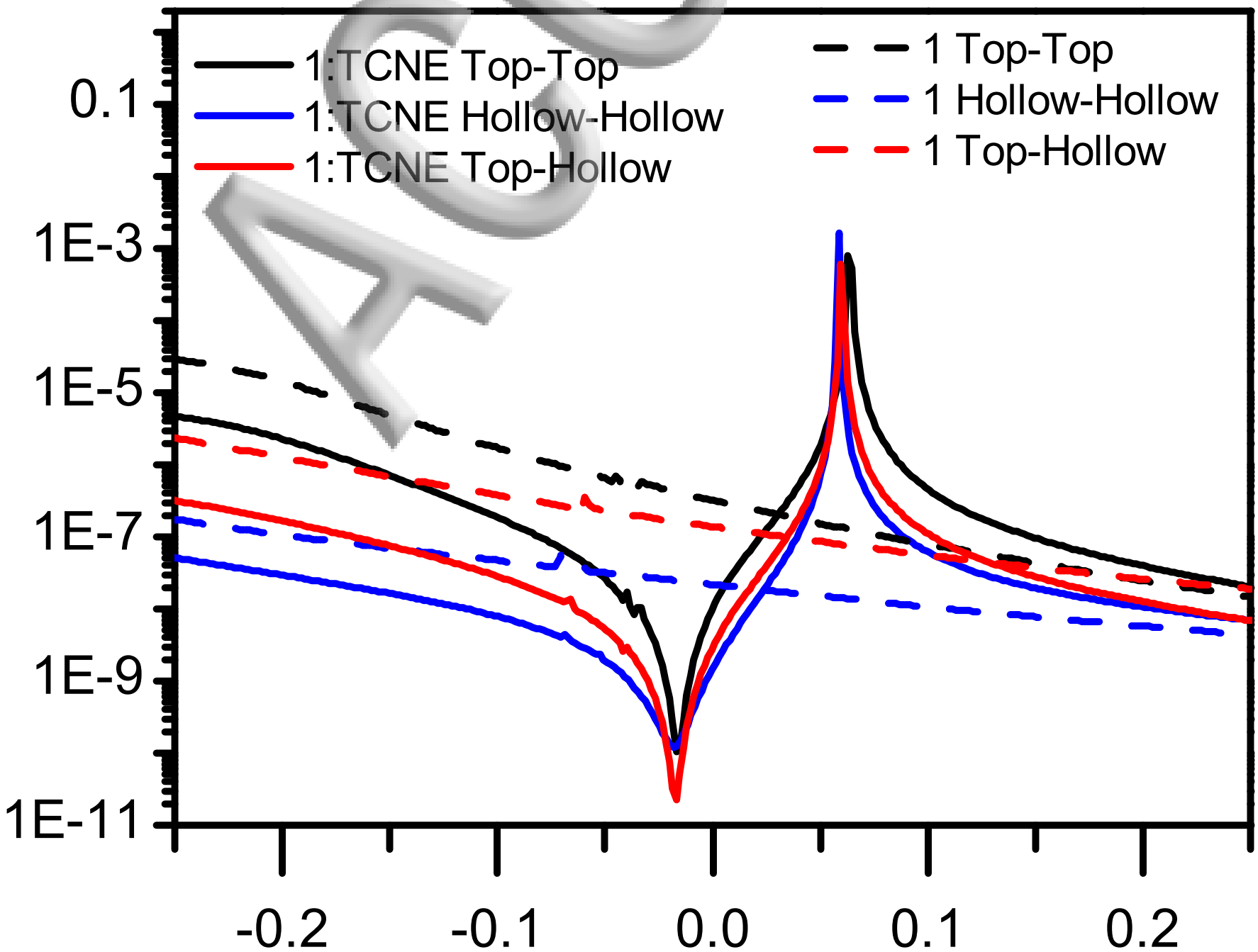
1:TCNE Top-Top
1:TCNE Hollow-Hollow
1:TCNE Top-Hollow
1 Top-Top
1 Hollow-Hollow
1 Top-Hollow
0.1
1E-3
1E-5
1E-7
1E-9
1E-11
-0.2
-0.1
0.0
0.1
0.2